World Journal of Engineering and Technology, 2023, 11, 874-892
https://www.scirp.org/journal/wjet
ISSN Online: 2331-4249
ISSN Print: 2331-4222

Design and Optimization of Actuator for HT-25 Multifunctional Loader

Md. Al Imran Tapu[1*], Joy Howlader[2], Md. Shahriar Sujan[1], Md. Jahangir Alam[3], Md. Mehedi Hassan[4]

[1]College of Harbor Coastal & Offshore Engineering, Hohai University, Nanjing, China
[2]Department of Computer Science and Technology, College of Computer and Information, Hohai University, Nanjing, China
[3]College of Civil and Transportation Engineering, Hohai University, Nanjing, China
[4]Department of Information Communication Engineering, College of Internet of Things, Hohai University, Nanjing, China
Email: *tapu.imran@outlook.com, shahriarsujan16@gmail.com, joyhowlader007@gmail.com, jahangiralam504016@outlook.com

How to cite this paper: Tapu, Md.A.I., Howlader, J., Sujan, Md.S., Alam, Md.J. and Hassan, Md.M. (2023) Design and Optimization of Actuator for HT-25 Multifunctional Loader. *World Journal of Engineering and Technology*, **11**, 874-892.
https://doi.org/10.4236/wjet.2023.114058

Received: January 15, 2023
Accepted: November 24, 2023
Published: November 27, 2023

Abstract

To break down the development interaction of the working gadget of the multi-practical wheel loader and to compute the heap of each part, the Denavit-Hartenberg strategy was applied to build up the kinematics of the instrument model. Also, all the while, set up the elements model of dynamic framework. A multi-body element programming MSC, ADAMS and its active module were applied to assemble component power through a pressure framework reenactment model. An entirety working cycle interaction of the functioning gadget of the wheel loader was mimicked, and the investigation results thoroughly show the development interaction of the functional device and the stacked state of each part, and check the mechanical properties of the working gadget and dynamic execution water-driven framework effectively.

Keywords

Multifunctional Loader, Hydraulic Circuit, CAD, Power System, Hydraulic Actuator and Pump

1. Introduction

For great portability and flexibility, the multi-utilitarian loader is utilized in practically every limited-scale earthwork site, and it is a commonplace variable burden mechatronic item. The customary plan technique dependent on the physical model makes the long plan pattern of the multi-practical loader, which can't adjust to changes on the lookout. Assembling the actual model will expand the expense of a multi-practical loader plan, and it restricts the improvement of the loader. The rise of virtual prototyping innovation takes care of the issues of conventional plans. With this innovation, designing staff can straightforwardly utilize the actual data and mathematical data of different parts given by the CAD framework, like mass, a snapshot of latency, and so forth. The multi-practical loader can be gathered on the PC to acquire a virtual model, and the model can be reenacted afterwards. We can completely comprehend the actual properties of the loader before it is created. The reproduction results are the premise of a limited component examination of key segments. We dissect the commonplace working gadget of a multifunctional loader with dynamic investigation programming ADAMS. We assemble reenactment models of mechanical and water-powered frameworks of the functioning gadget. The models can mimic real working conditions and various work on this premise. Dynamic recreation of mechanical and hydraulically powered frameworks of the functioning gadget should be possible in the stacking measure. We will contemplate the exhibition of the working gadget throughout the whole working cycle, like shift qualities, programmed level execution, and release execution. We can likewise examine the unique exhibition of a powered framework with a pressure-driven module given by ADAMS, making the reproduction results more precise. The energy utilization of rough terrain vehicles, for example, wheel loaders, chiefly rely upon the energy productivity of their transmission frameworks, which typically embrace persistent variable transmission (CVT) to improve the solace. Flow innovations permit the following CVT arrangements: hydrodynamic transmission (force converter), hydrostatic transmission (HST) (water-driven siphon/engine), mechanical transmission, and electric transmission. The hydrostatic transmission is a hydraulic drive with a closed (closed) circuit, which includes one or more hydraulic pumps and motors. In Russian and Soviet literature, hydraulic transmission is another name for this type of hydraulic drive. "The most frequent use of a hydrostatic transmission is the drive of a wheel or traverse machine device—where the hydraulic engine is designed to transmit mechanical power from a drive motor to a bridge, wheel or star driven by a tracked machine. Adjusting pump feed and output traction power due to hydraulic motor control [1] [2]. Hydrostatic transmission has many advantages over mechanical drive. One of the advantages is the simplification of mechanical wiring by car." This allows you to gain reliability because you cannot tolerate and repair the car with a large load on the card and car. In the northern conditions, it occurs more often at lower temperatures [3] [4]. Due to the simplification of the mechanical layout, it is possible to free up space for auxiliary equipment. Hydrostatic transmission can remove shafts and bridges, replacing pumping installations and hydraulic models with gearboxes embedded directly in the wheels. In a simple embodiment, hydraulic motors can be built into the bridge [5]. The first of the schemes mentioned where the hydro motors are embedded in the wheels may apply to the wheel machine, but more interesting in such hydraulic lines for tracked technology [6] [7]. For such machines, Sauer-Danfoss has developed a system of control systems based on hydraulic pumps and hydrometers of the 90 Series, H1 Series and Series 51 [8] [9]. The microcontroller control allows integrated control on the machine [10], starting from the diesel engine control [11]. During operation, the system ensures side synchronization for straight lines of the strings and onboard rotations of the machine with a helmet or electric joystick [12]. The second project mentioned above is used for tractors or other wheels. It is a hydraulic device consisting of a hydraulic pump and motor built into the leading bridge [13]. "To control the hydraulic drive, mechanical or hydraulic control can be used, and the most advanced electrical control technologies can be used using the controller built into the hydraulic pump. The program for controlling such hydraulic engines can be installed separately in the MC024 microcontroller" [14]. For dual-way, it allows you to control the hydrostatic transmission, and the engine can live. Electrical control allows you to provide a more smooth and accurate adjustment of the speed of movement and the traction power of the machine. "The disadvantage of hydrostatic transmission cannot be considered high efficiency, which is significantly lower than mechanical transmission. However, hydrostatic transmission can be more profitable and faster than mechanical transmissions with gearboxes. This is during manual gear shift; it must be given a gas pedal and pressed. The engine consumes a lot of power, and the car's speed is changing with the jolt. All of this negatively affects both speed and fuel consumption. In hydrostatic transmission, this process is uninterrupted, and the engine operates in a more profitable mode, which increases the stability of the entire system" [15].

2. Power Train Schematic

The water-driven framework incorporates two variable uprooting siphon/engines: one as siphon Unit 1 to communicate the motor force through the pressure-driven lines and another as engine Unit 2 to send water-driven capacity. They open pressure relief valves when the hydraulic system reaches unsafe or excessive levels. High pressure without valves can give a hose or literally "blow" except for a hydraulically driven motor or cylinder. Static pressure relief valves are commonly used as protection devices for any additional pressure situation.

Some safety valves are made as a one-time device and need to be replaced when they perform the task. Others can reuse time and time again to release high-pressure fluids. Some static pressure release valves may allow the fluid to be re-discharged into the reservoir tank for reuse, while smaller hydraulic systems may release the fluid outside the sealed system (**Figures 1-3**).

The power train for a wheel loader ought to have the option to deal with the most extreme applied wheel force [15] (**Figure 4**).

3. Designing Multi Loader

3.1. Introduction Loader Attachment

HT-25J multi-useful loader is a heavy-duty tool that can be set aside or loaded with materials such as pitch, debris, snow, dirt, food, gravel, logs, raw materials, recycled materials, rock, sand, wood chips, etc. ...cabin comprehensive view,

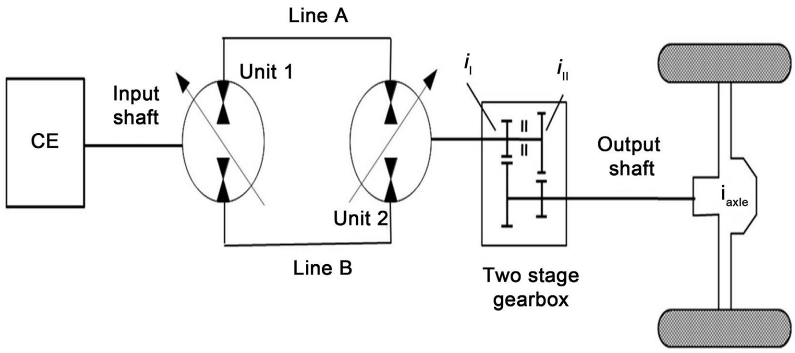

Figure 1. Hydrostatic transmission (HST).

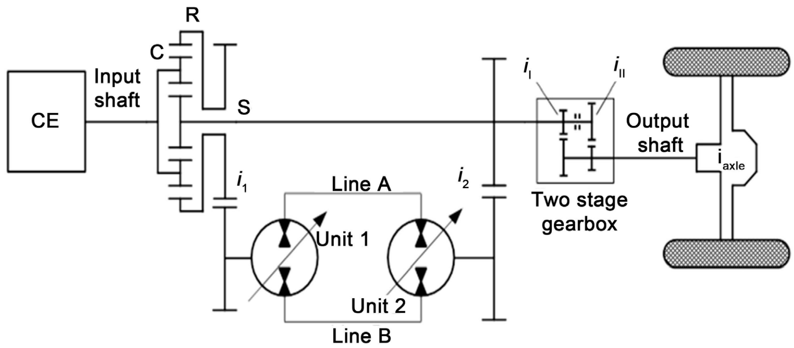

Figure 2. Power split transmission (PST).

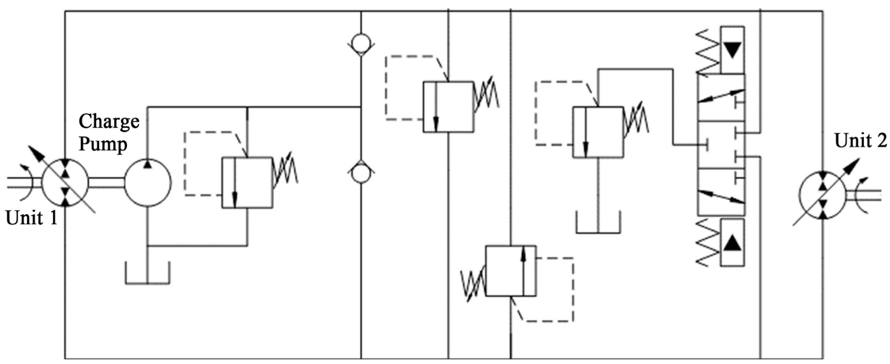

Figure 3. Hydraulic circuit.

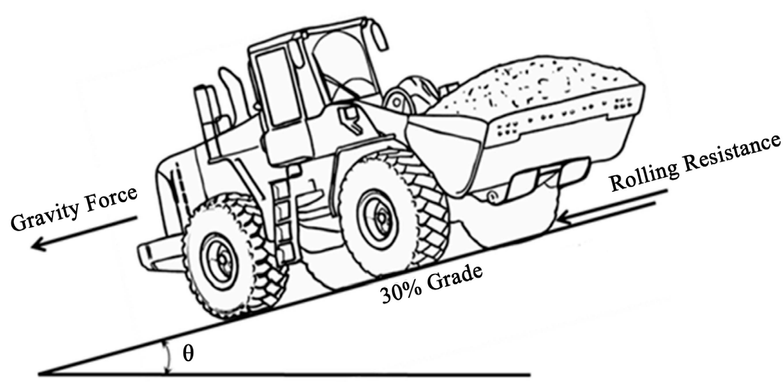

Figure 4. Wheel loader.

comfortable and air-conditioned cabin, driving system four-wheel drive [15] (Figure 5).

3.2. Working Principle and Modelling

3.2.1. Multi-Directional Display of Wheel Loader

1) High quality, reliable guarantee of industry-leading production equipment and process quality;

2) Optimal design, strong generality of main parts;

3) The choice of hydraulic transmission and hydraulic torque converter, power transmission more reliable and more flexible operation;

4) Larger wheelbase, reasonable bridge load distribution, large traction force and lifting power, good machine form and operation stability;

5) The liquid oil and hydraulic oil tank layout is reasonable, and the hood is opened to the side for convenient maintenance. Low-pressure wide-base cross-country tires are adopted, and the rear axle can swing up and down around the centre, so it has cross-country performance and passing performance and is suitable for ragging driving and operating roads;

6) The pin sleeve adopts a sealing structure, which can prevent dust and dirt and improve the service life;

7) Tone structure, small turning radius, flexible turning adoption, and work with narrow space;

Likewise, we planned three connectors that permit changing an engine's direction, as portrayed in Figure 3. The split connector can fundamentally expand the number of potential designs whenever embraced with the 90˚ connector (Figure 6).

3.2.2. Demonstrating Measure

The framework is based on the following coordinates component relevant matrix following.

$$A_i = \begin{bmatrix} \cos\theta & -\sin\theta\cos\alpha & \sin\theta\sin\alpha & a\cos\theta \\ \sin\theta & \cos\theta\cos\alpha & -\sin\alpha\cos\theta & a\sin\theta \\ 0 & \sin\alpha & \cos\alpha & d \\ 0 & 0 & 0 & 1 \end{bmatrix}.$$

For bucket orientation, the equation is

$$T_2 = A_1 A_2$$

A_1 —boom relative to the base.

A_2 —bucket relative to the boom.

The coordinates of the bucket tooth tip are as follows.

$$\begin{bmatrix} x \\ y \\ z \\ 1 \end{bmatrix} = T_2 \begin{bmatrix} 0 \\ 0 \\ 0 \\ 1 \end{bmatrix} = \begin{bmatrix} a_2c_1c_2 - a_2s_1s_2 + a_1c_1 \\ a_2s_1c_2 + a_2c_1s_2 + a_1s_1 \\ 0 \\ 1 \end{bmatrix}$$

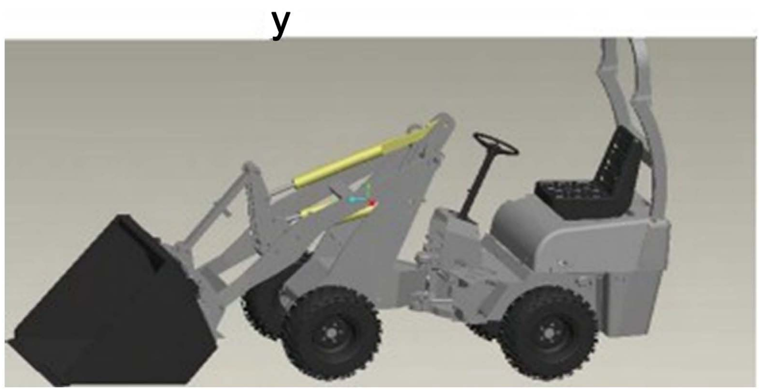

Figure 5. HT25J Loader model.

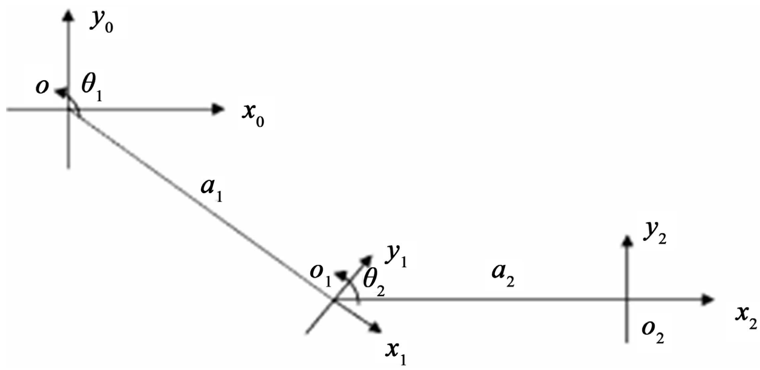

Figure 6. D-H coordinate diagram.

$$\begin{cases} x = \left(a_2c_1c_2 - a_2s_1s_2 + a_1c_1\right)x_0 \\ y = \left(a_2s_1c_2 + a_2c_1s_2 + a_1s_1\right)y_0 \end{cases}$$

and $z = 0$.

3.3. Materials and Methods

Upon completion, the study concludes that there are two primary mechanisms for the vehicle with multifunctional loaders. The necessities mentioned above are the multifunctional loaders. Firstly, the power supply must be designed as a small hybrid system. The problems include the layout of the force, the engine and the battery module. Secondly, the device should be hydraulic to reduce engine load. The power is provided by the battery module, which is the hydraulic system. Each module has its hydraulic valves built into a hydraulic valve block to simplify the design and decrease staff time. Starting as a shock and transport equipment, the device module is ready to transport soil slumbering and soil that can be quickly utilized for disaster relief. The vehicle can be extended to various agricultural operations, including ploughing and spraying through the established order of replacement modules.

3.4. Mobile Loader Module

Standard locomotion mode can be grouped into three categories: wheeled type, multi-pedal articulated type and tune type. Roller cars are the most common, with low-cost blessing and noise, easy manipulation, and the ability to ride high speed on flats.

Brakes and sensors are, therefore, essential additives to this device. The stability of the gadget control is also a problem, in addition to the complex shape and the excessive value. Vehicles used in marine and civil engineering are typically tracked. The blessings are minor reinforcement stress, overall performance on the right side of the road, strong capacity to cross limitations and dikes and relative power for transport. Tracked vehicles can rotate in the area with a tiny standard rate turning radius. The tracked cars are more adapted to catastrophic relief than the two other types and are therefore chosen as a multifunctional loader mode with the aid of such a study.

3.5. Hybrid Power System Design of the Loader

The mild-hybrid gadget for energy is divided into classes: the ISG, the integrated starter generator, and the Belt Starter Gadget (BSG) [16]. The ISG system is blessed to have a quick reaction speed and a clean movement. The BSG gadget uses a hybrid parallel energy production, which uses an EM to fuel the ICE crankshaft with a serpentine belt. **Figure 7** shows the EM unit mounted within the role of a traditional vehicle alternator. This technique is cheap for achieving small hybrid strength functions, including engine beginning and foresting, power help and mild renewable braking packages. This was valued and pursued by many car companies [17]. The BSG system was changed into an additional method for this observation after evaluation. It is also of low value, in addition to the gain that no more unique changes were required to the ICE structure. As a result, the loader power unit is designed to convert into the motor mode for slim space operations to decrease the amount of exhaust in the area around the vehicle, carry out reduction blessings and improve overall vehicle performance. If the battery is low and the drives are powered simultaneously as the curtain drives the generator to recharge the battery, the gadget is changed to engine mode. The machine is turned into a hybrid strength mode while an enormous torque output is required. The ICE and EM torques are joined together for high torque outputs.

Because the state-of-the-art charging process can significantly extend the Li-ion battery cycle life, Li-ion batteries have been selected as an electric-powered energy supplier/store [18] [19]. The Li-ion battery offers the engine and the hydraulic pump power, and the hydraulic gadgets are driven to actuate by the hydraulic valve. The machine can start the engine or change the force into the transmission system through the loader vehicle via a loading belt. The engine is motorized. **Figure 8** shows the structure of the hybrid energy machine.

3.6. Drive Specifications Design of HT-25 Multifunctional Loader

At some stage of regular avenue driving, distinguishing road surfaces and loads

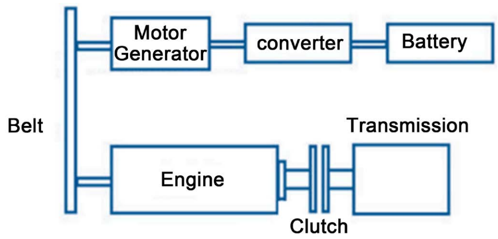

Figure 7. Generator structure of belt-starter.

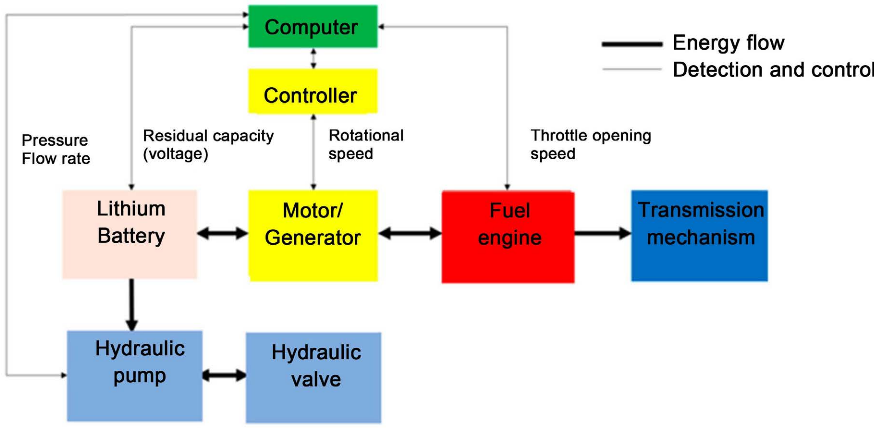

Figure 8. Design of hybrid power system.

are first considered accelerating, de-escalating and mountain adjustments. The load can be split into fully loaded and unloaded weights during design. The unloaded weight shows the importance of general mini-farming tanks with a weight of 280 kg, and a whole load is the weight of the hydraulic cylinder system alongside the 480 kg device module. The average person on foot is considered for the moving speed layout of the car from 3.85 - 5.44 km/h, and the highest speed is 4.2 km/h. The power system layout is decided by calculating the most power needed in car use as shown in the following equation, to ensure that the car can perform in extraordinary circumstances [20].

$$p \geq \frac{1}{\eta_r}\left(\frac{mgf_r}{3600}V_{\max} + \frac{C_d A}{76140}V_{\max}^3\right).$$

In this equation, force p within the left dimension is the consumption of strength to overcome resistance. On the right-hand side the situation of natural electric vehicles refers to. Natural electric cars can be driven at their highest speed under the right conditions, which is why the desired strength should not be much lower than the electricity amount and the kinetic car's resistance. F_r is the drag coefficient similar to the deformation of the ground; $V_{\max}$ has the highest speed and η_r It is the coefficient of transmission. The wind resistance is not noted because the highest tour rate of this examination is ready to slow down. The equation is streamlined as follows:

$$p \geq \frac{1}{\eta_r}\frac{mgf_r}{3600}V_{\max}$$

The loader weighs 730 kg while the loader is loaded fully on a standard road floor. The loading performance of the tracked cargo is 0.9, and the track-to-floor strength is 0.18; the absolute loaded maximum velocity is 3.2 km/h, which is to take on the following values: m = 730 kg, f_r = 0.18, η_r = 0.9, and $V_{\max}$ = 3.2 km/h. Then the equation becomes:

$$\text{p} \geq 0.9895 \text{ KW}$$

When the loader reaches a slope at a certain speed, the equation of power consumption is shown as follows:

$$p \geq \frac{1}{\eta_r}\left(\frac{mgf_r \cos\alpha}{3600}V_{\max} + \frac{\text{mgsin}\alpha}{3600}V_{\max} + \frac{C_d A}{76140}V_{\max}^3\right)$$

Due to slowing the speed, the wind can remove power consumption. Then it is like the equation:

$$p \geq \frac{1}{\eta_r}\left(\frac{mgf_r \cos\alpha}{3600}V_{\max} + \frac{\text{mgsin}\alpha}{3600}V_{\max}\right)$$

When the loader is fully loaded, the climbed slope reduces the maximum speed for security issues to 2.5 km/h. Then, m = 730 kg, f_r = 0.18, η_r = 0.9, and $V_{\max}$ = 3.2 km/h can be replaced by p as follows:

$$\text{p} \geq 3.4687 \text{ KW}$$

This value suggests that the required energy for travelling flat is over 0.969 kW and more than 3.4687 kW for climbing slopes. The drive machine of this examination desires an additional 3.505 kW to ensure that the loader can be used in various situations. The data is given in Table 1.

3.7. Generator/Motor

Power required for fully loaded driving on a flat ground is $\text{p} \geq 0.9895 \text{ KW}$ in segment F, and the energy necessary for fully loaded electric power on a pitch is $\text{p} \geq 3.4687 \text{ KW}$. "The engine (MC016) is 1.6 kW and can be used for flats". Furthermore, it exceeds the design requirement of 3.4687 kW. The overall torque is good at 3500 rpm, and the data is given in Table 2.

3.8. Battery Pack

There is little need for car power system battery systems. Therefore, for Li-ion battery systems (26,650, Life Cell Battery Fty., Guangzhou, Guangdong, China), 15 battery cells were first connected to a collection. Then, six agencies were linked together to produce a percentage of the 48 V/12 Ah battery from Table 3. At the same time, the system was used to generate battery packing. The battery pack supplies the motor, hydraulic pump and solenoid valve with electricality. Table 3 provides parameters for a single cellular battery.

3.9. Hydraulic System and Tool Modules Designing

This layout employed a power-pushed electric hydraulic pump to omit greenhouse gas emissions from ICE. The hydraulic pump (Smiths Hydraulics) has

Table 1. Multifunctional loader performance index.

Vehicle Weight (Empty)	480 kg
Power of the Drive System	≥3.5 kW
Load Capacity (Maximum)	280 kg
Unloaded maximum speed on standard routes	4 km/h
Fully loaded maximum speed on standard roads	3.5 km/h
Highest Degree	35%
Speed at the highest degree	3.2 km/h

Table 2. Specifications of motor.

Item	Data
Structure of motor	internal rotor
Type of motor	PMSM
Voltage	40 - 58 V
Method of cooling	Air cooling of Natural type
Weight	6.35 kg
Power rating output	1.6 kW
Rational speed ratings	3500 rpm
Torque rating	4.606 Nm
Maximum output capacity	4.5 kW
Highest Speed	5400 rpm
Highest Torque	Nm

Table 3. Parameters of the battery cell.

Battery Type	$LiFePO_4$
Voltage rating (V)	3.33
Capacity rating (mAh)	2350
Current highest level of continuous discharge (C/A)	30/70
Current Maximum Discharge Impulse (C/A)	50/120
Maximum voltage for charging (V)	3.7
Output Cut-off Voltage (V)	2.5
Current charging (C)	10
Weight (g)	75
Life of Cycle (count)	1600 2200

decided to use electricity from DC according to the design goal. Current operators can adjust rotational speed, glass speed, and fluctuation rate by handling the current. The rated output is 2.7 kW, in line with the pump specifications. It can produce 3 kW, the working pressure can reach 190 bar at a most current 170 A, and the system can move to 2.606 c.c./rev at a maximum current. Table 4 shows unique specifications. The hydraulic pipeline layout is illustrated in Figure 9.

3.10. 3D Modelling of the HT-25 Multifunctional Loader

The mechanical design of the automotive loader module and hybrid energy machine is completed using CAD software, as illustrated in Figure 10, in line with loader characteristics and size assessment findings. In the first place, the modules capable of moving the cars are the driving wheel, the wheel assistant, the track chain, the wheel manual and the track tracks. The transmission gadget's gearbox is associated with the loader's mobile module following the power wheel. The engine and the hydraulic pump are then brought. The pinnacle, including the engine, gas tank, engine, generation unit and lithium battery, is after the hybrid strength platform. Figure 11 shows the designs of this hydraulic system and the necessary device modules in the excavation module.

4. Test of the Hydraulic Pump System and Hybrid Power System

The hybrid strength system includes testing the engine, hybrid strength and battery mode. In the flowchart shown in the figure, the measures concerned in the checkout of engine mode are given. 13. First, exam confirmation of the activation of the engine's gasoline valve and the coil spark plug switch. The controller is on, and the motor's rotary path is confirmed. As the motor rotates, the motor ignites and starts correctly. The motor is activated. A dipstick checks whether gasoline is sufficient when the engine does not go on. Then, the engine starts, stops, and is turned on by a generator to keep the battery loaded. For charging batteries, this look limits modern charging maximum to 7 amps and units of increased charging mode while state-of-the-art charges (SOC) are lower than 70%.

Figure 12 shows the measured charging current. During rotation, the engine uses about 12 - 14 amps of electricity. When the engine is shut down, it turns into a generator, and the electricity for charging is 7 amps. At 35 s, the electricity charging drops unexpectedly. The aim is to tie up the embrace and move forward with the low gear, which only slows down rotational speed. The electricity can be kept at 7 amps utilizing the throttle (Figure 13).

Flowchart:

The hybrid mode controls the motor and the motor at the same rotational speed to increase the torque. The test method is nearly the same for hybrid and motor modes. The handiest difference is that after the engine begins, the system controls the motor and motor at the same rotational speed; when a velocity difference occurs, the power output worsens. The control process for the motor power mode is similar to that for the motor and hybrid power mode. If the residual battery capacity throughout the motor mode is less than 60 percent, the device switches mechanically to motor mode to help charge the battery. Although the potential residual is greater than 90%, the gadget switches to motor mode

Table 4. Parameters of the hydraulic pump system.

Output Rating (kW)	2.5
Voltage of operation (V)	24
Highest Current (A)	170
Highest Output (kW)	2.7
The pressure of working (bar)	190
Displacement of system (cc/rev)	2.606

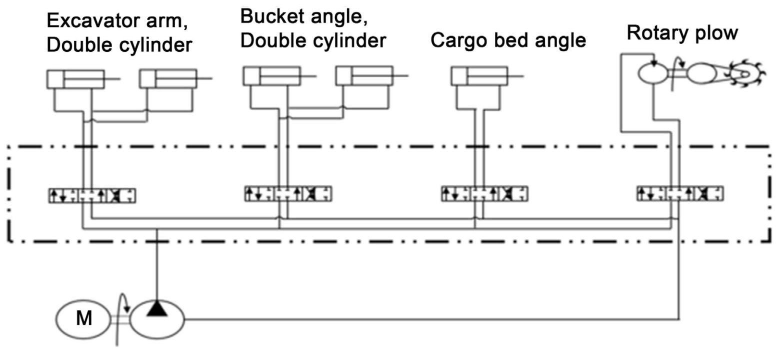

Figure 9. Design of the hydraulic pipeline.

Figure 10. 3D diagram of the HT-25 Multifunctional loader.

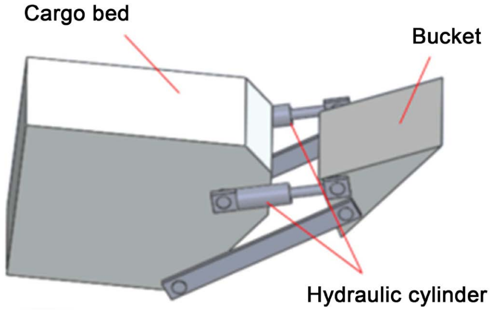

Figure 11. 3D diagram of the tool module and hydraulic system.

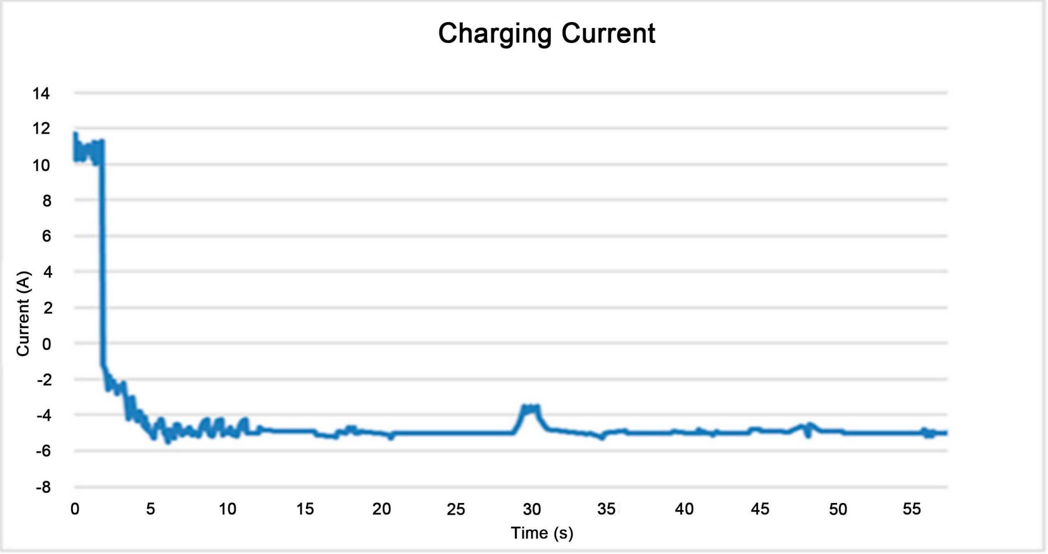

Figure 12. Charging of the battery module by motor.

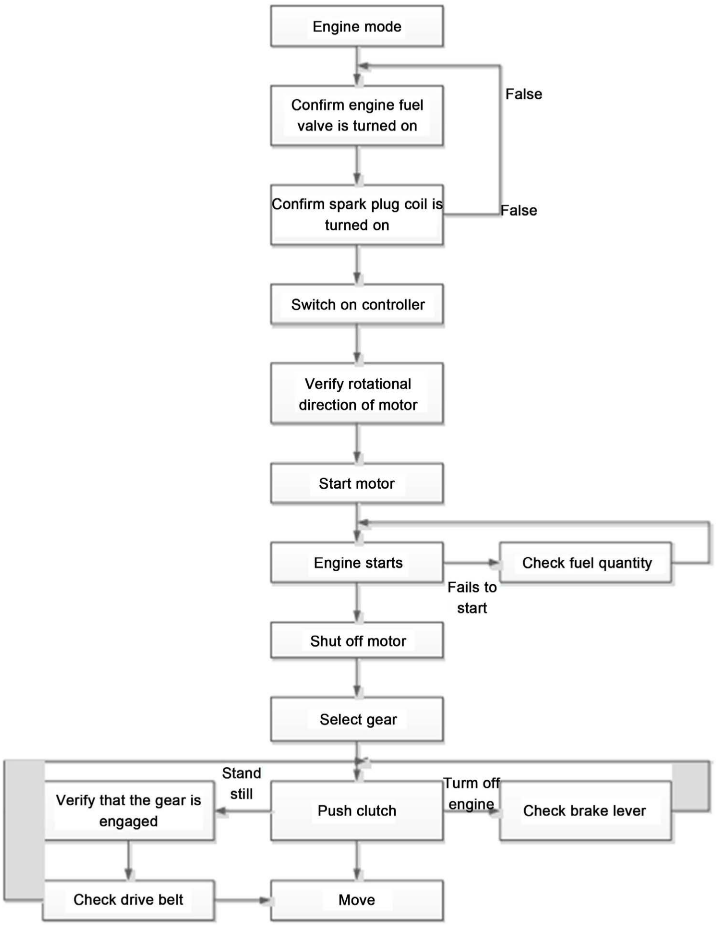

Figure 13. Flowchart of the engine mode system.

again. The battery's residual potential and the usable time are determined as follows:

$$\text{SOC} = \frac{\text{battery charge}}{\text{charge after charging is completed}}$$

The SOC is 60%, the load remains 12 Ah after charging is complete, and the average electricity of the motor is 10 A. **Figure 14** shows the experimental report. As a result, the battery used for 4.8 Ah and 28.8 min can be calculated. This means 100% to 60% of the engine battery can run constantly for about 30 minutes. Charging the battery takes about 40 minutes after replacing the motor to assess the 90% residual capacity.

5. Mechanism of the Actuator System Using ADAMS

The HT-25 multifunctional loader connector can be built on a virtual prototype simulation model with Pro/E and ADAMS. For one thing, the three-dimensional modelling software Pro/E can be made for each CAD component. The model has specific physical properties, like mass inertia moment. Then, we can put the pieces together in an entire working device model. The model as the whole operating device may be imported with the Mechanical/Pro software interface module provided by ADAMS. ADAMS/Hydraulics are typically simulated to interact mechanically and hydraulically and specify system motion characteristics so that several static, modal, and transient analyses are completed. Hydraulics and ADAMS View share the same library functions and parametric functions. Hydraulic components can be designed using DS, DOE, and OPTIMIZE. Hydraulic diagram modellers can be used to create hydraulic circuit models in hydraulics. It employs an open data structure, and the hydraulic components required can be chosen from a library.

Last but not least, hydraulic components will be linked parallelly. Dynamic hydraulic and mechanical system equations are fully coupled, making the integrator more efficient in solution. The loader works with the cylinders and boom cylinders. In this study, the boom loop and the bucket loop with ADAMS/Hydraulics module are determined using the same pressure source, making simulation results more accurate. The model includes hydraulic oil, tank, hydraulic cylinders from the pressure source, check valves, directive valves, valves, and hydraulic tubes (**Figure 15**).

1) Oil for hydraulic purposes, 2) Source of pressure, 3) Control valves, 4) Tank, 5) Valve directional steering, 6) The connector of the circuit, 7) Valves, 8) Cylinder boom, 9) Cylinder bucket.

The booming loop and the seal loop are provided with the hydraulic system. The boom-slip cylinder and cylinders in mechanical systems can be switched by controlling the valve in the loop. The step function in ADAMS Hydraulic is used to manage the valve, and it works as follows:

The control system of the cylinder bucket:

STEP (time, 2.1, 0.1, 2.2, −1.1) +

STEP (time, 4.2, 0.1, 4.3, 1.1) +
STEP (time, 8.5, 0.1, 8.6, 1.1) +
STEP (time, 9.9, 0.1, 9.8, −1.1)

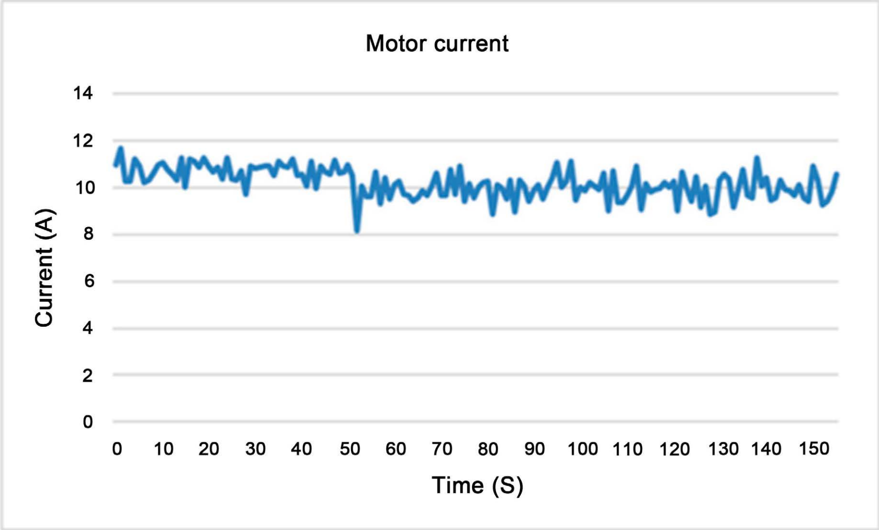

Figure 14. Measured current consumed by the motor while discharging.

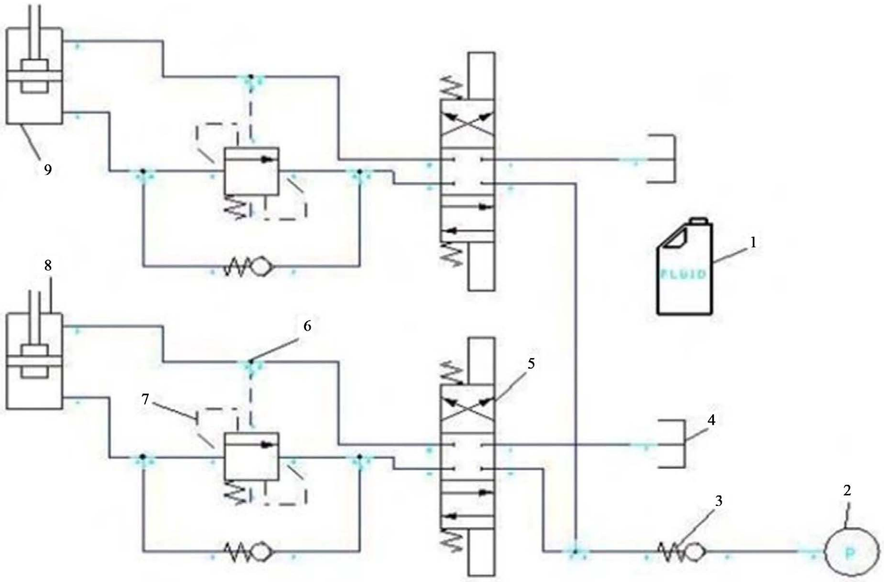

Figure 15. Circuit Diagram of the hydraulic bucket and boom.

The control system of the cylinder boom:
STEP (time, 4.5, 0.1, 4.6, 1.1) +
STEP (time, 8.3, 0.1, 8.6, −1.1) +
STEP (time, 10.1, 0.1, 10.3, −1.1) +
STEP (time, 12.3, 0.1, 12.5, 1.1)

The cylinder speed determines the working device efficiency, and the cylinder extension length determines the bucket's position at different times. The rate of the two cylinders piston and the size of the cylinders must be studied (**Figure**

16).

The change in elongation of the two cylinders after completing a working cycle is minimal, as seen from the curve. After the work is completed, the functional

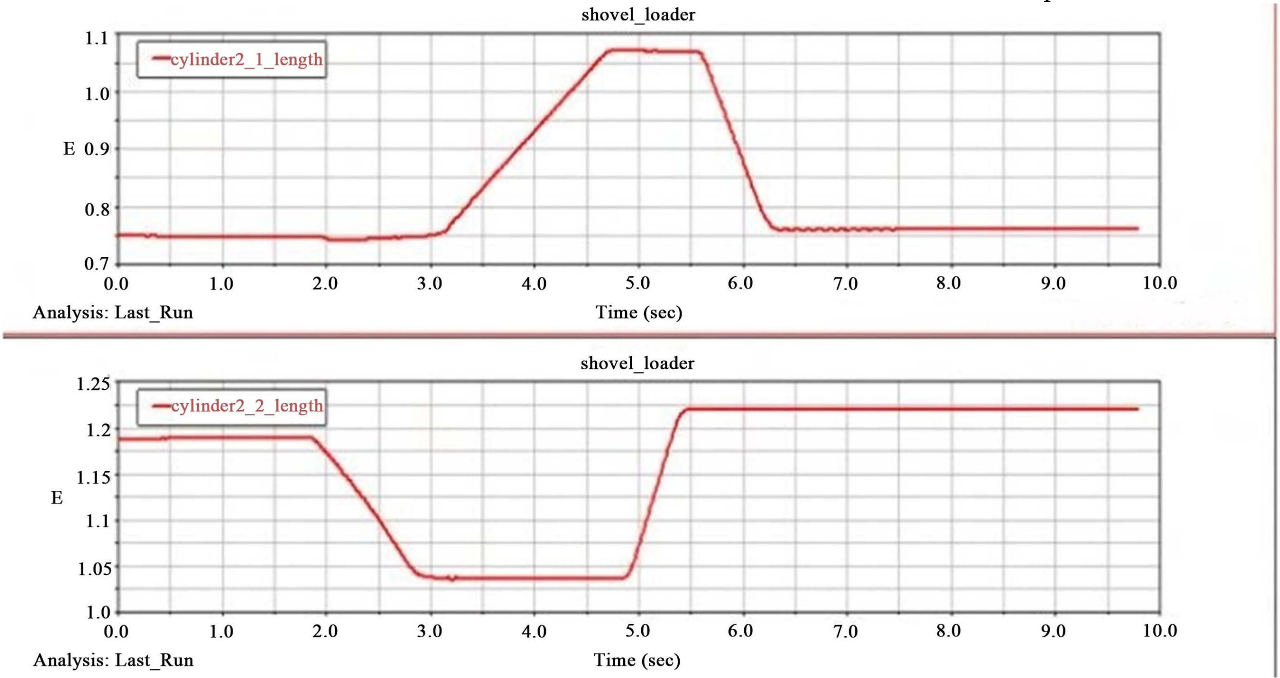

Figure 16. Cylinder bucket and cylinder boom length curve.

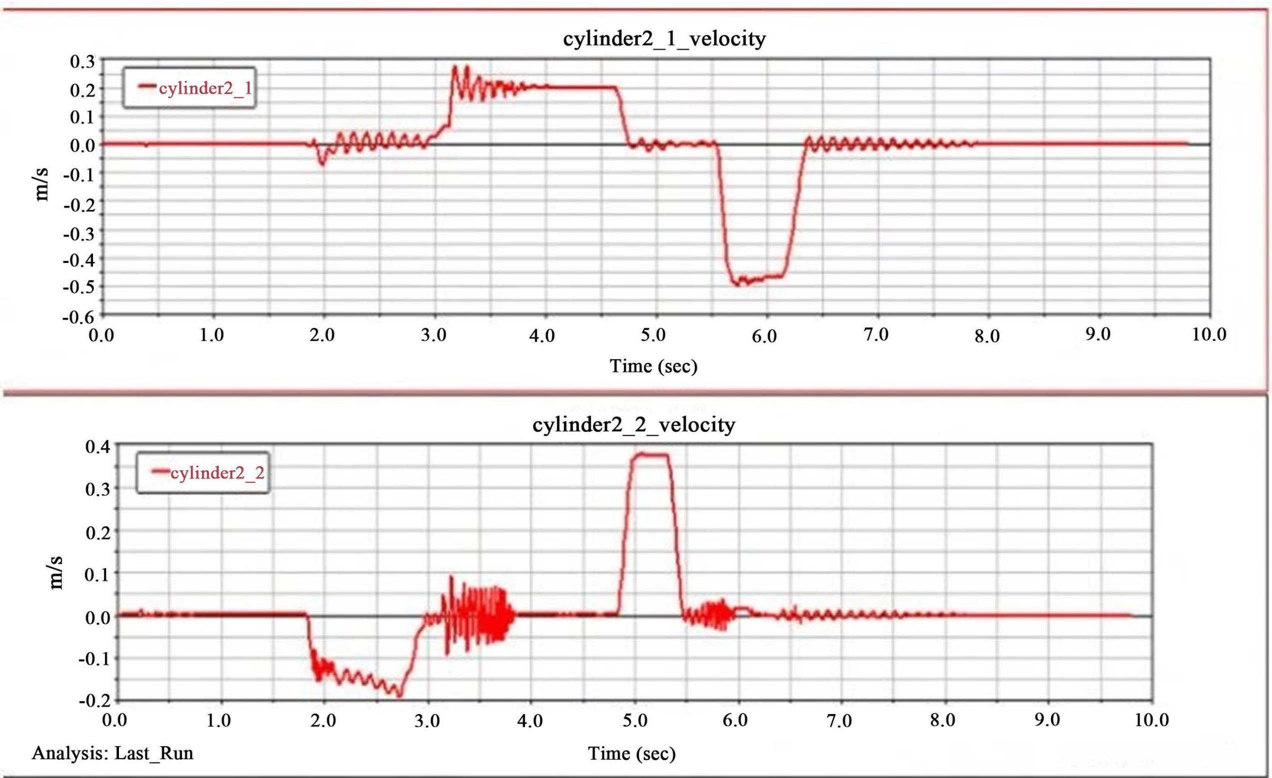

Figure 17. Cylinder bucket and cylinder boom speed curve.

device can be flat automatically. When the cylinder begins to act at 2 seconds, the two-cylinder speeds are fluent throughout the bucket process. Therefore, the loading of external loads significantly influences the cylinder speed. The rate of

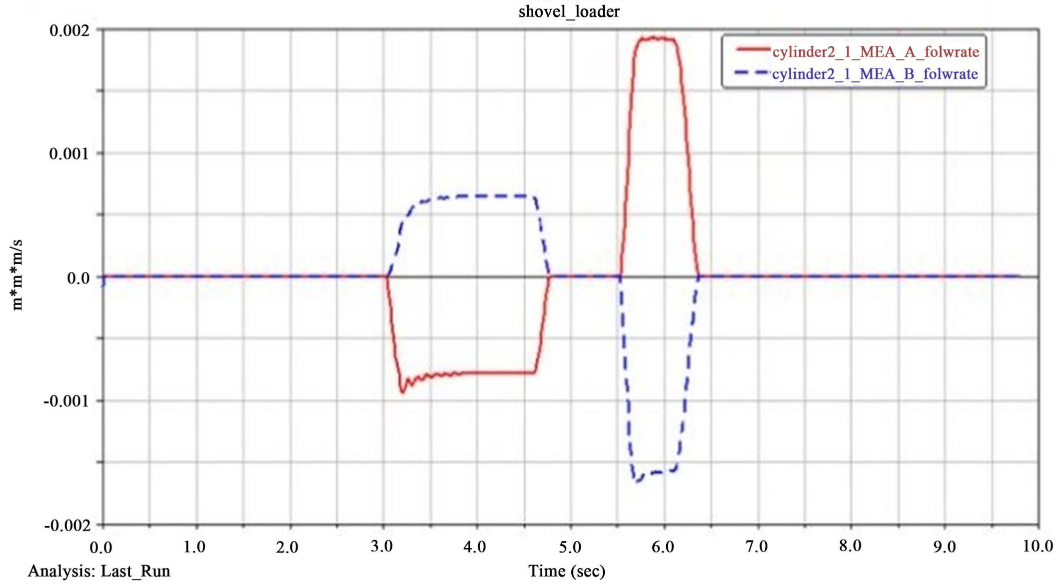

Figure 18. Cylinder boom flow curve.

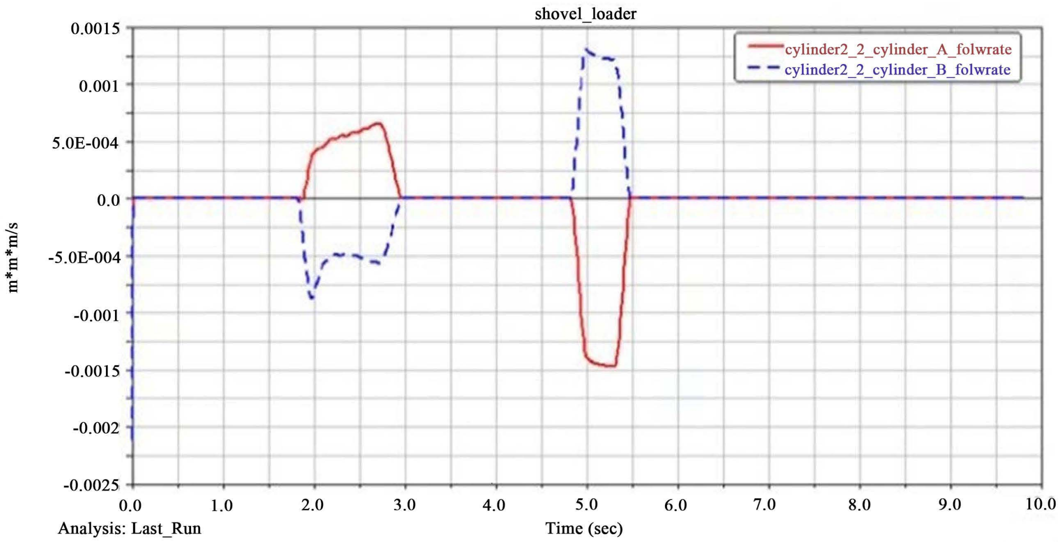

Figure 19. Cylinder bucket flow curve.

both cylinders during the boom is relatively stable. The work equipment returns to the initial position after unloading. Both cylinders are slightly fluctuated and are finally stabilized (Figures 17-19).

6. Conclusion

This study discusses the design and optimization technique for the actuator of HT-25 multifunctional loader. AutoCAD did the designing of the necessary things. The whole process and calculation are done technically, making it very cost-effective. The system acquires the best energy efficiency by matching the engine's power and the electric motor. The loader has a very operator-friendly working environment. It can work in any narrow space also. The system's best feature is that it is less polluter of air. So, it is very environment friendly also. Here, electricity is used instead of gasoline fuel. So, there are no greenhouse gas emissions from the system.

Conflicts of Interest

The authors declare no conflicts of interest regarding the publication of this paper.

References

[1] Macor, A. and Rossetti, A. (2011) Optimization of Hydro-Mechanical Power Split Transmissions. *Mechanism and Machine Theory*, **46**, 1901-1919. https://doi.org/10.1016/j.mechmachtheory.2011.07.007

[2] Comellas, M., Pijuan, J., Potau, X., Nogués, M. and Roca, J. (2013) Efficiency Sensitivity Analysis of a Hydrostatic Transmission for an Off-Road Multiple Axle Vehicle. *International Journal of Automotive Technology*, **14**, 151-161. https://doi.org/10.1007/s12239-013-0017-z

[3] Jarchow, F. (1964) Leistungsverzweigte Getriebe (Power Split Transmissions). *VDI-Z*, **106**, 196-205.

[4] Kress, J.H. (1968) Hydrostatic Power-Splitting Transmissions for Wheeled Vehicles—Classification and Theory of Operation. SAE Technical Paper 680549. https://doi.org/10.4271/680549

[5] Carl, B., Ivantysynova, M. and Williams, K. (2006) Comparison of Operational Characteristics in Power Split Continuously Variable Transmissions. SAE Technical Paper 2006-01-3468. https://doi.org/10.4271/2006-01-3468

[6] Nilsson, T., Fröberg, A. and Åslund, J. (2012) Fuel Potential and Prediction Sensitivity of a Power-Split CVT in a Wheel Loader. *IFAC Proceedings Volumes*, **45**, 49-56. https://doi.org/10.3182/20121023-3-FR-4025.00017

[7] Liu, X.J., Sun, D.Y., Qin, D.T. and Liu, J.L. (2017) Achievement of Fuel Savings in Wheel Loader by Applying Hydrodynamic Mechanical Power Split Transmissions. *Energies*, **10**, Article 1267. https://doi.org/10.3390/en10091267

[8] Macor, A. and Rossetti, A. (2013) Fuel Consumption Reduction in Urban Buses by Using Power Split Transmissions. *Energy Conversion and Management*, **71**, 159-171. https://doi.org/10.1016/j.enconman.2013.03.019

[9] Schulte, H. (2007) Control-Oriented Modeling of Hydrostatic Transmissions Considering LEAKAGE Losses. *IFAC Proceedings Volumes*, **40**, 103-108. https://doi.org/10.3182/20071029-2-FR-4913.00018

[10] Kim, H., Oh, K., Ko, K., Kim, P. and Yi, K. (2016) Modeling, Validation and Energy Flow Analysis of a Wheel Loader. *Journal of Mechanical Science and Technology*, **30**, 603-610. https://doi.org/10.1007/s12206-016-0114-9

[11] Zhang, H., *et al.* (2016) The Optimization Design of a New Type of Hydraulic Power-Split Continuously Variable Transmission for High-Power Tractor. *Journal of Nanjing Agricultural University*, **39**, 156-165.

[12] Park, Y.J., Kim, S.C. and Kim, J.G. (2016) Analysis and Verification of Power Transmission Characteristics of the Hydromechanical Transmission for Agricultural Tractors. *Journal of Mechanical Science and Technology*, **30**, 5063-5072. https://doi.org/10.1007/s12206-016-1056-y

[13] Do, H. and Ahn, K. (2012) A Study of Energy Saving Hydraulic System by a Pressure Coupling Hydrostatic Transmission. *Journal of Drive and Control*, **9**, 10-17. https://doi.org/10.7839/ksfc.2012.9.1.010

[14] Zhang, Q. (2008) Basics of Hydraulic Systems. CRC Press, Boca Raton. https://doi.org/10.1201/9781420071023

[15] Xiong, S., Wilfong, G. and Lumkes Jr., J. (2019) Components Sizing and Performance Analysis of Hydro-Mechanical Power Split Transmission Applied to a Wheel Loader. *Energies*, **12**, Article 1613. https://doi.org/10.3390/en12091613

[16] Baldizzone, S. (2012) Performance and Fuel Economy Analysis of a Mild Hybrid Vehicle Equipped with Belt Starter Generator. Master's Thesis, University of Windsor, Ontario.

[17] Steffan, R., Hofmann, P. and Geringer, B. (2015) Potentials of a 48 Volt Belt-Starter-Generator in the Powertrain of an Ultra-Light Vehicle. SAE Technical Paper 2015-01-1155. https://doi.org/10.4271/2015-01-1155

[18] Chen, P.T., *et al.* (2019) Reviving Aged Lithium-Ion Batteries and Prolonging Their Cycle Life by Sinusoidal Waveform Charging Strategy. *Batteries & Supercaps*, **2**, 673-677. https://doi.org/10.1002/batt.201900022

[19] Chen, P.T., *et al.* (2018) Moderate Energy for Charging Li-Ion Batteries Determined by First-Principles Calculations. *Batteries & Supercaps*, **1**, 209-214. https://doi.org/10.1002/batt.201800052

[20] Hsiao, Y.H., *et al.* (2016) A 77-GHz 2T6R Transceiver with Injection-Lock Frequency Sextupler Using 65-nm CMOS for Automotive Radar System Application. *IEEE Transactions on Microwave Theory and Techniques*, **64**, 3031-3048. https://doi.org/10.1109/TMTT.2016.2604304